Rapid Kimberlitic Fluid Extraction from the Lithospheric Mantle

I.J. BASSON
Dept. of Geological Sciences
Univ. of Cape Town, Rondebosch 7701
e-mail: ibasson@geology.uct.ac.za

H. JELSMA
CIGCES, Dept. of Geological Sciences
Univ. of Cape Town, Rondebosch 7701
e-mail: jelsma@cigces.uct.ac.za

G. VIOLA
Dept. of Geological Sciences
Univ. of Cape Town, Rondebosch 7701
e-mail: gviola@geology.uct.ac.za

Introduction

Kimberlite and related rocks range in age from the Archaean (evidence for diamonds in the Witwatersrand Basin and in Ghana; phlogopite-rich lamprophyre in the Kuruman area of the Kaapvaal Craton; Janse, 1985; Bristow *et al.*, 1986) to Recent (Leucite Hills in Wyoming and the Eiffel area of Germany; Janse, 1985). Carbonatites and kimberlite occurrences become more abundant from the Proterozoic onwards, and remarkably more abundant from approximately 600 Ma onwards (Janse, 1985; Dawson, 1986; Wolley, 1989; Lubala, 1991; Haggerty, 1989, 1994; Harmer, 1998), partly due to their erosion-prone nature and ongoing crustal uplift and evolution. The most notable post-Pan-African peak in **kimberlite volcanism** occurred in the mid-Cretaceous (**approx. 124-83 Ma**) in southern Africa, North America, Brazil and Siberia, areas that display a 200 Ma subsidiary kimberlite intrusion peak (Skinner *et al.*, 1992; Haggerty, 1994). Kimberlite intrusion events in the southern Africa region are directly comparable to **carbonatite intrusion events** in the same region; approximately 679-491 Ma (essentially Pan-African) and **139-116 Ma in Angola, Zimbabwe, Malawi, Tanzania and South Africa** (Wooley, 1989). While Janse (1985) cites approximately **19 kimberlite-/lamproite-forming events**, Dawson (1986) approximates **16 events or phases worldwide**. A total of **4 main events are proposed for southern Africa** (Dawson, 1986; Skinner *et al.*, 1992; Fig. 1).

To date over **780 kimberlites have been found in southern Africa** (Smith, 1983; Smith *et al.*, 1985; Gurney *et al.*, 1991; Skinner *et al.*, 1992; White *et al.*, 1995). Mesozoic southern African kimberlites are divided into 2 groups on geochemical and mineralogical grounds (Smith *et al.*, 1985); **145-115 Ma (mainly Group II)** and **95-80 Ma (mainly Group I)** (*op. cit*). Group I kimberlites, which are "normal" ilmenite-bearing kimberlites and have distinct Pb, Sr and Nd isotopic ratios, also intruded at approximately 1600 Ma, 1200 Ma, 500 Ma; Group II kimberlites are highly-micaceous and ilmenite-poor (*op. cit.*). While carbonatitic activity increased with time, it is episodic and temporally & spatially associated with major orogenic events (Woolley, 1989); i.e. the **"localization of carbonatitic activity over time / several periods suggests lithospheric control"**, furthermore, **"the location and genesis of carbonatites [and carbonatitic activity] is determined in some way by the physical and/or chemical properties of the lithospheric plate"**; supported by van Straaten (1989), **"carbonatite magmatism is related to recurrent reactivation of older structures and argues for a control by crustal rather than mantle processes."**

Cretaceous Events

- Increased mid-Cretaceous mantle convection (**"superplumes"**; Larson 1991a, b; Ricciardi and Abbott, 1996; Haggerty, 1994).
- **Accelerated plate motion** coincided with the arrival of the Parana, Etendeka, Gondwana and Ontong Java Superplumes, representing a deep-sourced heat pulse from the CMB and coinciding with a "Normal" geodynamo field orientation between 120 and 80 Ma (Haggerty, 1994).
- **Higher mean mantle Potential temperatures** (PTs), temperatures skewed towards higher values and a greater degree of temperature variance, (Ricciardi and Abbott, 1996); increased rate of global mantle convection and plate motion (*q.v.* Sharp, 1974; Hartnady and le Roex, 1985; le Roex, 1986; Larson, 1991a, b; Hill, 1991; Haggerty, 1994). A more regular potential mantle temperature resumed after *ca.* 73 Ma or just after the end of the mid-Cretaceous (*op. cit.*).
- Kimberlites erupted **prior to 90 Ma** (nominally Group II types) sampled mainly **harzburgitic material from depths between 180 and 140 km**, within a **210-220 km thick lithosphere** with a geotherm of 34 $mW.m^{-2}$ (Smith, 1983; Smith *et al.*, 1985; Brown *et al.*, 1998).
- **Post-90 Ma** kimberlites sampled a **highly metasomatised lithosphere**, raised geotherm of 40 $mW.m^{-2}$, from shallower depths (**170 km**; *op. cit.*).
- A **mid- to late-Cretaceous spike in sediment volume** in the offshore Natal-Mozambique and Orange Basins (Summerfield, 1996; Brown *et al.*, 1998; 1990; Botha and de Wit, 1996).
- **Extreme thinning of the MBL**, significantly raised geotherms and uplift driven by buoyancy, resulting from a decrease in the density of the lithospheric roots (*q.v.* Brown *et al.*, 1998; 1990), causing a mid-Cretaceous global sea-level highstand (e.g. Summerfield, 1996).
- **Uplift and denudation**, constrained by apatite fission-track (FT) dating. A 101 ± 10 Ma FT apatite age for rocks outcropping at Luderitz (Namibia), 96 ± 7 Ma and 103 ± 8 Ma FT apatite ages 50 km east of the western southern African margin, a relatively poorly constrained age of 140 ± 16 Ma at Aus (approximately 100 km from the western margin) and an age of 83 ± 6 Ma at 200 km from the western southern African margin (Summerfield, 1996; Brown, 1992; Brown *et al.*, 1990).
- **"Vertically coherent deformation"** (Silver *et al.*, 2001) wherein changes in the lithospheric mantle are reflected in the overlying upper lithosphere.

Cretaceous Plate Motion

- Data summarized in Summerfield (1996), in turn based on data from Duncan (1981), Morgan (1983), Hartnady and le Roex (1985) and le Roex (1986), depict a **"U-turn" between 150 and 50 Ma**, wherein **plate motion** swung **from W** (relative to present African azimuths) **to SW** (*q.v.* Online Goddard Space Flight Centre, VLBI Sol. KB2001 of Version 01).
- Recent summaries of African Plate motion spreading vectors (Müller *et al.*, 1993; Dalziel *et al.*, 2000; University of Austin, Texas data; Lawver *et al.*, 2001), calculated from mid-ocean ridge studies: 140 Ma to 60 Ma showed **unusual characteristics, compared to pre-145 Ma and post-60 Ma motion** (Figure 1a). The direction of spreading (degrees from north) of the plate oscillated greatly; approximately 220° at 135 Ma, 140° at 125 Ma, 210° at 115 Ma, 145° at 100 Ma, 195° at 90 Ma to 160° at 60 Ma (*op. cit.*); this "oscillation" overlapped with a 135-100 Ma low-velocity period, with an average half spreading rate of about 6 $mm.yr^{-1}$, followed by a 95-60 Ma period wherein the half spreading rate doubled.

Model

1
2
- Consistent plate motion direction and velocity; development of preferred olivine alignment (*q.v.* present Kaapvaal Craton Ivrea zone fabric/LPO), melt orientation parallel to σ_1, coarsening of melt pockets, esp. from 184 Ma onwards (Karoo Basalt event). Precursor stresses to "U-Turn"/slowing down/rapidly varying plate motion direction (60/30 Myr periodicity).

3
- Phase of relatively poorly constrained motion, wherein plate vector oscillated (or continental U"-Turn", imposing σ_1 at high/obtuse angles on pre-existing melt; rapid (Incremental? Staggered?) readjustment of effective dihedral angle and expulsion of low-volume carbonatitic/kimberlitic fluids from thin mantle layers, necessarily accompanied by very rapid deformation of the lithospheric mantle (oscillation of <10 Myr periodicity). Note velocity "kick" at 100 Ma (*c.f.* changes in lithospheric mantle at approximately 90 Ma). Possible imposition of rapid deviatoric stress at high/obtuse angles to trends defined by Verncombe & Verncombe (2002), providing repeated/long-lived hosts for kimberlite/carbonatite intrusion (fluid expulsion in < 3 hours).

4
- Resumption of constantly changing plate motion vector and more regular plate velocities. Re-establishment of mantle fabric in <10 000 years – LPO currently evident from seismic studies.

Objectives

To clarify and summarize the sequence of events operative in southern African kimberlite intrusion, and the time-spans, periodicity and overlap of these events.

To merge recent data on a number of apparently unrelated features, such as plate motion vectors, lithospheric mantle fabrics and preferential mantle melt accumulation within these fabrics, with a view to explaining the mechanism of unusually abundant, geologically instantaneous kimberlite emplacement in the southern Africa region during the Mesozoic.

Kimberlite Emplacement Rates

Reference	Basis	Upper mantle-lower crust transit ΔZ = 100-10 km fluid velocity ($km.hr^{-1}$) *mins transit* **hours transit**	Transit speed within the upper crust as dykes ΔZ = 10-1 km fluid velocity *mins transit* **hours transit**	Fluidised intrusion as diatremes ΔZ = 1-0 km fluid velocity *mins transit* **hours transit**
McGetchin (1968) Model **M**	Fluid dynamics, Bernoulli equation, Newtonian flow in pipe	**(219)** ***(25)***	-	-
McGetchin (1968) Model **M**	Fluid dynamics, Bernoulli equation	-	**(669)** ***(0.8)***	-
McGetchin (1968) Model **M**	Fluid dynamics, Bernoulli equation	-	-	**(1998)** ***(0.03)***
McGetchin (1968) Model **F**	Fluid dynamics, Bernoulli equation, Newtonian flow in pipe	**43** ***29***	-	-
McGetchin (1968) Model **F**	Fluid dynamics, Bernoulli equation	-	**122** ***4***	-
McGetchin (1968) Model **F**	Fluid dynamics, Bernoulli equation	-	-	**(482)** ***(0.1)***
Ferguson (1970)	Flow in kimberlite dykes	-	**72** ***7.5***	-
Currie and Ferguson (1970)	Structural analysis, propagation of lamprophyre dykes	-	**72** ***7.5***	-
McGetchin and Ullrich (1973)	Fluid dynamics	**72-90** ***75-60***	-	-
McGetchin *et al.* (1973); Ullrich (1969)	Fluid dynamics and phase relations of carbonatitic and kimberlitic fluids	**200-20** ***29.7-297*** 0.5-4.95		
Smyth and Hatton (1977)	Preservation of diamond and coesite in lower transit area	***Several hours***	-	-
O'Hara *et al.* (1971); Mori and Green (1975)	Equilibration of mechanical mixture of water and mantle minerals	**100-4** ***NA*** 1-24		
Mercier (1979)	Recrystallization rates of strain-free neoblasts which replace strained crystalline mantle material	**40-70** ***150-85*** 2.5-1.4		
McCallister *et al.* (1979)	Exsolution in clinopyroxene	**11-25** ***545-240*** 9.1-4		
Ganguly (1981)	Kinetic diffusion calculations on pyroxenes and Ca-poor amphiboles	**0.7-0.01** ***NA*** 144-8544		
Mitchell (1979), Canil, Fedortchouck (1999), Rutherford and Gardner (2000)	Mafic dyke mineralogy, garnet dissolution rates (based on 160km thick lithosphere of Mitchell *et al.*, 1998)	**16-160** **375-38** 6.3-0.6		

Kimberlite Trends?

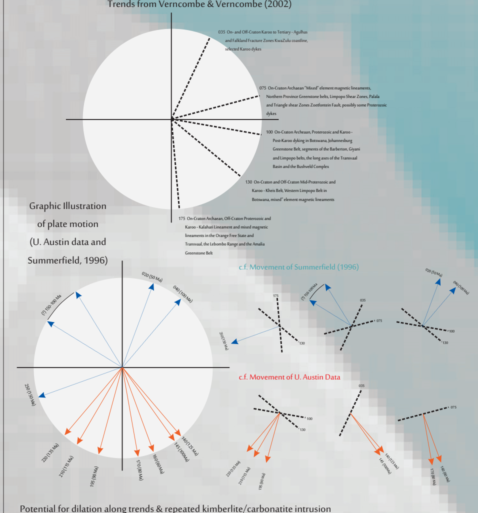

Conclusion

Plate still-stands, relative plate still-stands and plate motion velocity or vector changes provide for rapidly oscillating deviatoric stresses, which have a profound effect on mantle fabrics and preferred melt accumulation. Transmission of stress into the upper mantle must be extremely rapid to overcome grain-scale recrystallization ("Otswald ripening") rates, especially in the case of CO_2-H_2O fluid:matrix systems.

Lithospheric Mantle Structure

- Localized feeders of the Bushveld Complex (contains Premier kimberlite) (e.g. Viljoen, 1999); **cratonic root unscathed** i.t.o. diamond potential.
- A N50E-(approximately NE-) **trending shear wave splitting** (fast) **polarization direction** evident from a closely-spaced broadband array across the Kimberley area (Vinnik *et al.*, 1995; Fouche *et al.*, 2001).
- Parallels **"central EET high"**, an "arcuate saddle-like maximum (average width >> 350 km, average magnitude >> 70 km) from northeast to southwest [which] dominates the EET map" (Doucouré and de Wit, 1998).
- The central EET high coincides with **present-day velocity vector of the African plate** (*q.v.* Vinnik *et al.*, 1995), N40-45E at 14-20 $mm.yr^{-1}$ (Online Goddard Space Flight Centre, VLBI Solution KB2001 of Version 01).
- Trend coincides with **the spatial** (but not temporal?) **Venetia-Premier-Kimberley kimberlite trend** (*c.f.* Hartnady and le Roex, 1985; le Roex, 1986; Skinner *et al.*, 1992), and NE-SW lithospheric extensional stress of up to 8 MPa at approximately 125 km depth (Doucouré and de Wit, 1998).
- **Two mutually orthogonal lattice preferred orientations pervasive throughout the Ivrea Zone** (LPO) (Ben-Ismail *et al.*, 1998, 2001):
  1) strongly plastically deformed and sheared with a high degree of deformation/recrystallization, possibly only locally formed by high-temperature asthenospheric diapers and **2)** c.g., commonly garnet-bearing, without microstructural signs of high temperature, stress or deformation rates; equilibrated at normal continental geotherms between 60 and 130 km, representative of the Archaean cratonic root.
- McKenzie (1979), Ribe (1989) and Vinnik *et al.* (1995) suggest seismic anisotropy of the mantle depends on the LPO of olivine, in turn caused by finite strain from simple shear. The [100], [010] and [001] axes in olivine become aligned with the longest, shortest and intermediate strain ellipsoid axes; maximum principal stress direction (σ_1) sub-perp. to 010 faces of olivine crystals (*q.v.* Waff and Faul, 1992); similar to oceanic crust, [100] axes oriented sub-parallel to spreading direction in the upper mantle (Christensen, 1984; Silver and Chan, 1988).
- Pearson *et al.* (1995) and Shirey *et al.* (2001) suggest no major thermotectonic event since Archaean times. Vinnik *et al.* (1995) suggested that the **present "flow"** or shearing of sublithospheric mantle of the Kaapvaal Craton (e.g. Ribe, 1989) is **inherited from Precambrian** or related to consistent plate motion the Jurassic period; a situation similar to the North American Craton (e.g. Ribe, 1989; Ruppel, 1995).

Mantle Melt Accumulation

- The measured effective dihedral angles for basaltic melt in contact with olivine range from 20° to 50°: for a wide range in melt fractions and dihedral angle, natural melt forms an interconnected network.
- **Increasing melt fraction and increasing grain size results in an increase in the size and aspect ratio of melt pockets**, (usually parallel to the 010 crystal faces of olivine); occurs under hotspot conditions (Daines and Kohlstedt, 1996; Crough *et al.*, 1980; Haggerty, 1994).
- The melt pocket aspect ratio (long : short axis ratio) is highest at low melt fractions (0.01 to 0.02: concurs with the partial melt fractions proposed for the generation of kimberlitic/carbonatitic magmas or melt fraction required for 50% of grain boundaries to be wetted; Hirth and Kohlstedt, 1995a, b; Johnson *et al.*, 1990; Riley *et al.*, 1990) & at higher melt fractions (>0.18).
- Melilititic, nephelinitic and carbonatitic (and kimberlitic) melts are **highly mobile** in the upper mantle/lithospheric mantle at very small melt volumes (<1%; e.g. Watson and Brenan, 1987; McKenzie, 1989; Harmer, 1998).
- Ave'Lallemant and Carter (1970) noted **preferred orientations of melt** in an anisotropically deformed lherzolite:melt system, deformed at strain rates of 10^{-5} s^{-1} and confining pressures of 2.5 GPa
- Bussod and Christie (1991) found **preferred orientation of melt 'slots'** along recrystallized grain boundaries at 30° to σ_1 in partially molten lherzolite deformed under hydrous conditions at confining pressures of 1.5 GPa, 900-1100°C and differential stress of 100-400 MPa.
- Daines and Kohlstedt (1996): samples deformed at differential stresses greater than 100 MPa exhibited **more melt in pockets at 15-20° to σ_1**; melt pockets oriented parallel to σ_1 were also a factor of 2 larger, longer and more elongate than those arranged perpendicular to σ_1.
- Shear deformation of olivine-basalt results in a **preferred melt orientation**: a differential stress of 170 MPa and a total strain of over 230% produces melt preferred orientation within 20° of σ_1 (*c.f.* Bussod and Christie, 1991, Faul *et al.*, 1994; Daines and Kohlstedt, 1996).
- **Daines and Kohlstedt (1996): the degree of melt-preferred orientation relates to the duration of a (relatively high) differential stress, rather than strain rate/total cumulative strain (recall the NE-SE oriented 8 MPa found by Doucoure and de Wit, 1998). Surplus melt pockets primarily occur and may be expelled where the semi-molten rock contains more than its minimum energy porosity, a situation that arises during the deforming/non-static or non-hydrostatic case.**

Sequencing